Research paper

Development of a footprint description tool utilizing SMEAR Estonia eddy-covariance data and footprint modelling in combination with remote sensed forest species and land cover data

Joonas Kollo, Allar Padari, Alisa Krasnova, Ahto Kangur and Steffen M. Noe*

Kollo, J., Padari, A., Krasnova, A., Kangur, A., Noe, S.M. 2023. Development of a footprint description tool utilizing SMEAR Estonia eddy-covariance data and footprint modelling in combination with remote sensed forest species and land cover data. – Forestry Studies | Metsanduslikud Uurimused 79, 90–104, ISSN 1406-9954. Journal homepage: http://mi.emu.ee/forestry.studies

Abstract. Understanding how forest ecosystems respond to environmental factors, particularly in the context of global climate change, is essential for devising effective mitigation strategies. This study focuses on quantifying the interaction between forest ecosystems and atmospheric gases. To achieve our objectives, we are using the eddy covariance (EC) flux method to measure air turbulence and gas concentrations above the forest canopy at the Station for Measuring Ecosystem-Atmosphere Relations (SMEAR) in southern Estonia. We apply a flux footprint (FFP) model to describe the spatial extent and position of the surface area contributing to the turbulent flux measurements. The FFP analysis provides valuable insights into the long-term changes in SMEAR Estonia, the FFP and its relationship with forest management and land use changes. Our findings reveal that the FFP area varies from year to year due to changes in wind speed and direction, affecting the contribution of different land cover elements to the overall FFP. The average changes in the FFP area at a height of 30 meters were approximately 4.9%, while those at a height of 70 meters were only 1.6%. Moreover, human activities, such as thinning and clear-cutting, influence the growing stock and increment of forest stands.

Key words: SMEAR, footprint, fluxes, forest ecosystem, forest management.

Authors' address: Chair of Forest and Land Management and Wood Processing Technologies, Institute of Forestry and Engineering, Estonian University of Life Sciences, Kreutzwaldi 5, 51006, Tartu, Estonia; *e-mail: steffen.noe@emu.ee

Introduction

Forest ecosystems are well known as powerful regulators of Earth's climate via their impact on the fluxes of matter and energy between the land surface and the atmosphere (Hari *et al.*, 2009). Therefore, it is crucial to understand how forest ecosystems react to environmental factors. Studies of global climate change, relations between forest ecosystems and atmospheric gases during the last decades have identified the interaction between the land surface and the atmosphere as one of the key

DOI: 10.2478/fsmu-2023-0014

factors (Baldocchi *et al*., 1988; Hari *et al*., 2009; Noe *et al*., 2011; Rebane *et al*., 2020) we need to understand in order to quantify mitigation strategies reducing actual and future climate risks.

It was proposed that increasing concentrations of carbon dioxide (CO_2) as well as other greenhouse gases (H_2O, CH_4, NO_x) change the behaviour of radiation energy in the atmosphere (Zhong & Haigh, 2013). Forests act as terrestrial carbon sinks and their role as active modulators of the atmosphere's radiative transfer and albedo by particle and cloud formation were reported (Kulmala, 2016; Kulmala *et al*., 2014; Spracklen *et al*., 2011; Ezhova *et al*., 2018). It was further reported that rising atmospheric CO_2 mixing ratios lead to increased carbon uptake by the terrestrial sink (Keenan *et al*., 2016). Changes in climate occur both as a result of natural variability and as a response to anthropogenic forcing (Hari & Kulmala, 2008). Disturbances in forests play a major role in carbon (C) dynamics (Amiro *et al*., 2010; Rebane *et al*., 2020). Anthropogenic and natural disturbances affect the C balance in forest ecosystems as well as stand development and growth.

Gathering continuous long-term data on atmospheric and forest ecosystem relationships is important for monitoring environmental changes (Hari *et al*., 2009; Noe *et al*., 2015, 2016). For continuous data collection SMEAR (Station for Measuring Ecosystem-Atmosphere Relations) was established in southern Estonia where hemiboreal mixed forests are prevalent (Noe *et al*., 2015). Previously, four measuring stations had been established in Finland (SMEAR I–IV) (Noe *et al*., 2015). SMEAR Estonia is using the eddy covariance (EC) flux method which is based on measuring air turbulence and the concentration of gases like CO_2, methane, or water vapour. The method relies on the assumption of horizontal homogeneity (Hari & Kulmala, 2008; Teets *et al*., 2018) within an area sensed by instrumentation. EC is a micrometeorological method favoured for estimating the C balance, net ecosystem exchange (NEE) as well as many other atmospheric gases (Bourtsoukidis *et al*., 2014; Teets *et al*., 2018; Mäki *et al*., 2019). EC measures air fluxes, atmosphere gases and C exchange of the whole forest ecosystem above the tree canopy (Baldocchi, 2003; Hari & Kulmala, 2008; Teets *et al*., 2018) and is the most used and common method to measure the turbulent air fluxes above the forest canopy (Vesala *et al*., 2008).

The flux footprint (FFP) model concept has been used since 1972, described by Schmid (2002) in his review paper. These models are used to describe the spatial extent and position of the surface area that contributes to a turbulent flux measurement at a specific point in time, for specific atmospheric conditions and surface characteristics (Kljun *et al*., 2015).

The flux tower gathers data from a certain distance that is called the source area or flux of the FFP. The FFP defines the field of view of the flux tower sensors and thus reflects the influence of the surface on the measured turbulent flux (Aubinet *et al*., 2012). The flux of the FFP is dependent on measurement height, surface roughness and thermal stability (Burba & Anderson, 2010). If a surface is homogeneous, the exact location of a sensor is not as essential as it would be if a surface were inhomogeneous because in the latter case the fluxes from all parts of the surface are, by definition, equal. If the surface is inhomogeneous, the measured signal depends on the part of the surface which has the strongest influence on the sensor, thus it affects the location, shape and size of the FFP (Schmid, 2002; Vesala *et al*., 2008; Chu *et al*., 2021). Flux is dependent on three main circumstances: 1) concentration of gases crossing the area; 2) size of the area; 3) the time it takes for gases to cross the area (Burba & Anderson, 2010; Chu *et al*., 2021). The FFP analysis and description has been recognised as a method when it comes to the establishment of the tower (Finnigan, 2004) to e.g. ensure the capture of the flux signal from the ecosystem of interest. We

propose to widen the angle and use a yearly timestep in re-analysing and describing the changes in the FFP of the SMEAR Estonia station that provides long-term data on ecosystem carbon exchange.

The main aims of the paper are 1) to assess the yearly FFP area and changes in the forest area, the growing stock, and growth increment related to the area that is given by the cumulative FFP covering 90% of flux signals measured at the height of 30 and 70 meters; 2) to assess the changes due to wind speed and direction changes of the FFP description and; 3) to relate and grade these changes with the inclusion of knowledge on forest management and land use changes. This results in a detailed description of the FFP which gives us ample opportunity for future research.

Materials and Methods

Description of the site

SMEAR Estonia (58.2714°N, 27.2703°E, 36 m a.s.l.) is situated at the Järvselja Experimental Forestry Centre. The forest ecosystem within the station's FFP is a hemi-boreal forest comprising, silver birch (*Betula pendula* Roth) and downy birch (*Betula pubescens* Ehrh.), Scots pine (*Pinus sylvestris* L.), Norway spruce (*Picea abies* (L.) H. Karst.), alder species (*Alnus spp.*), and common aspen (*Populus tremula* L.). The mean annual temperature in the area varies between 4 °C and 6 °C, the annual precipitation is 500–750 mm with about 40–80 mm as snow, and the growing season length is about 200–220 days (Noe *et al*., 2016; Kollo *et al*., 2023). The experimental site consists of a 130 m tall main flux tower, the main cottage for power supply, internet access, a storage for online data, and the pumping facilities and gas analysers for the flux tower (Noe *et al*., 2015). Different atmospheric greenhouse gases, such as carbon dioxide (CO_2), water vapour (H_2O) and methane (CH_4) are measured together with reactive trace gases, such as ozone (O_3), nitrogen oxides (NO_x = NO + NO_2) and sulphur dioxide (SO_2).

Flux data collection and the FFP calculation workflow

All flux data were collected at SMEAR Estonia (Noe *et al*., 2015) by continuous high-frequency (10 Hz) measurements (Noe *et al*., 2021). Raw data from the flux tower were stored at half-hour intervals and cover the years from 2015 to 2020. Half-hourly data files were organised into separate years as input data. The eddy covariance system consists of a sonic anemometer (METEK uSonic-3 Class A) and an infrared gas analyser (Licor LI-7200, Lincoln, NE, USA) deployed at two heights, 30 m and 70 m a.s.l. at the flux tower. Data to determine the FFP, horizontal wind direction (wd) and speed (u), for advection and diffusion of gases and particles in this region – the surface friction velocity (u*), the standard deviation of lateral wind speed deviations (σ_v), and Obukhov length (L) were obtained by using anemometer readings and applying EddyPro software (LI-COR, Lincoln, NE, USA). A set of basic parameters (Table 1) is needed to calculate the FFP plus the displacement height (d), which was chosen constant at 13.4 m determined by the average canopy height of the area and the measurement height above ground (zm) which depends on the height of the receptor – either 30 or 70 m.

Table 1. Basic input parameters and definitions for the Kljun *et al.* (2004) FFP model.

Input	Description
zm	measurement height above ground (m)
z0	roughness length (m)
d	displacement height (m)
u_mean	mean wind speed at zm (m/s)
L	Obukhov length (m)
sigma_v	standard deviation of lateral velocity fluctuations after rotation (m/s)
u*	friction velocity (m/s)

To calculate the annual FFP climatology, we used the stand-alone Python version of the FFP model (Kljun *et al.*, 2015).

The workflow of the FFP (Figure 1) calculation was as follows: using the Kljun FFP model (Kljun *et al.*, 2004, 2015) each year's FFP were calculated separately to get the area and shape of the FFP at the 10%, 50%, 60%, 70%, 80% and 90% contours of cumulative source weights (Figure 2). We chose these percentages to get a more detailed description of the FFP. We first filtered out all non-available (NaN) values, then eliminated data where friction velocity (u*) parameter was smaller than 0.2 to avoid the use of non-turbulent atmospheric conditions. The next step was checking wind direction values for proper range (0–360 degrees) and after that we created the needed input vectors for the Kljun model algorithm. Finally, we run the FFP algorithm to get the x-y distances from the tower for each contour, which then were saved separately for each year in csv format files to further use them as input to the geographic information system (GIS). For this work we used data measured at 30 and 70 m.

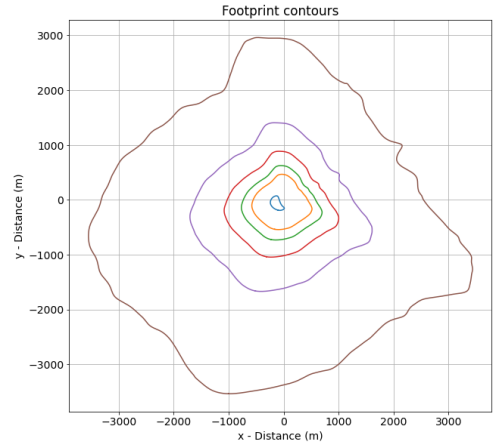

Figure 2. A representation of the cumulative FFP contours at the 10%, 50%, 60%, 70%, 80% and 90% contours of source weights for each year at the height of 70 m.

To compare to the annual FFP shape and area we assessed the annual heterogeneity of the horizontal wind regime. For that, we calculated the horizontal wind speed and direction density using Mathematica (Wolfram Research, Inc., Mathematica, Version 12.3.1, Champaign, IL, USA) for both measurement heights and each year of our experiment.

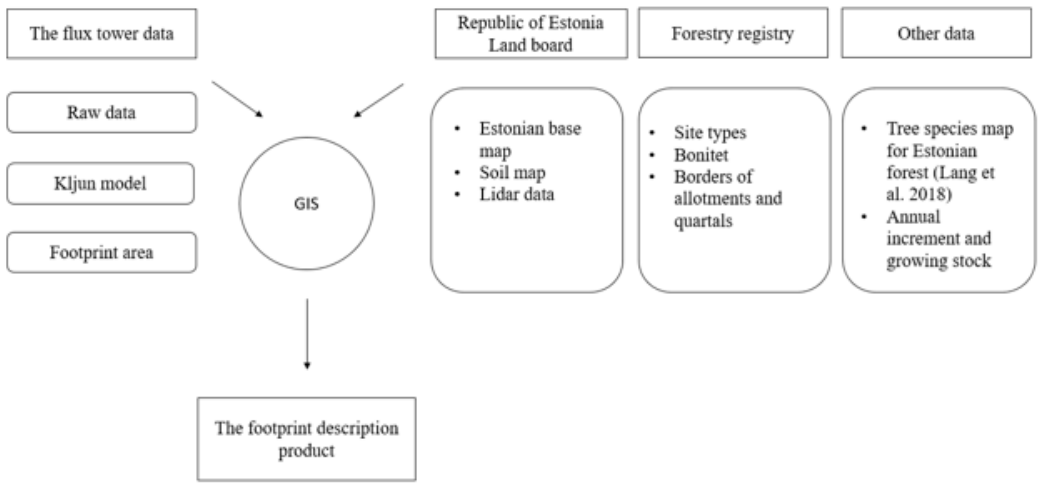

Figure 1. Scheme of the workflow to reach from flux tower raw data to the FFP description product.

Determining forest stand parameters and data

Basal data of forest stand parameters related with the stand height increment and volume stock are usually measured at 5-year intervals in Estonia. Remotely sensed LIDAR height measurements have a frequency of 4 years (https://geoportaal.maaamet.ee/). Therefore, it is necessary to assess the yearly figures of forest stand parameters by modelling that allows to map the years when no actual measurement took place.

We therefore modelled the increase in the height of all stand elements using the models for normal forest stands as proposed by Kiviste & Kiviste (2009). The volume stock was modelled by using the national regulations according to the Forest Inventory Act (2009).

Preparation of spatial data and land cover elements

To create a forest mask, we used everything from the woody vegetation layer of the Base Map from the Estonian Topographic Data Collection (Maa-amet, 2017) and added from the wetland layer the areas with woody vegetation (column PUIS_T contains the value "Yes"). Since the forest surface layer also contains the surface areas of infrastructure elements (roads, ditches, railways, power lines, and quarter boundaries) which are usually mapped in GIS layers as so-called "line type elements" with no spatial extent we needed to determine the surfaces of such line elements. Therefore, it was first necessary to generate for each line type a fitting surface type representing the area that can then be added as a new layer into the forest mask. In this work, we selected only the layers of line elements that are passing through forests. For this purpose, we introduced a layer of roads, layer of ditches, layer of railways, layer of power lines and a layer of forest quarter boundaries. For roads, ditches, railways, and forest quarter boundaries we used again information that can be retrieved from the Base Map. For power line routes we used data from the national transmission operators Elering and Fortum. To avoid possible double accounting, we deleted areas overlapping with the surfaces of line elements from the forest layer.

Results

The FFP description measured from a height of 30 m

The cumulated FFP covers a surrounding area of up to 600 m from the main tower if we use flux data measured at 30 m height (Figure 3). In 2015 the FFP covered 61.6 ha, in 2016 it covered 65.4 ha, in 2017 60.2 ha, in 2018 62.3 ha, in 2019 and 2020 the FFP covered areas of 61.4 ha and 58.3 ha, respectively. The average FFP area over the six-year period was 61.5 ha. The source area naturally depends on three main parameters: measurement height, wind speed and direction (Figure 3). However, the area is not only sensitive to the previous factors, but is also dependent on surface roughness and atmospheric stability (Vesala *et al*., 2008). The general shape of the FFP remained intact over the different years, although the FFP climatology is of a slightly different area for each year mostly due to changes in wind speed and direction. Figure 4 gives additional information on the density of wind data, where the darker colour shows a higher density of input data to the FFP model calculation. The FFP area in 2016 was 6.3% bigger than in 2015, but in 2017, it was smaller by 7.9% than in 2016. In 2018, the area was again bigger than in 2017 by 3.5% and was again smaller in 2019 than in the previous year by 1.5%. In 2020, the area was 5.0% smaller than in 2019. On average, the difference over the years was 4.8%. The smallest and the biggest area covered by flux data appeared to be in 2017 and 2020, respectively.

89.4 % of the FFP area regarding the 30 m high measurement point is covered

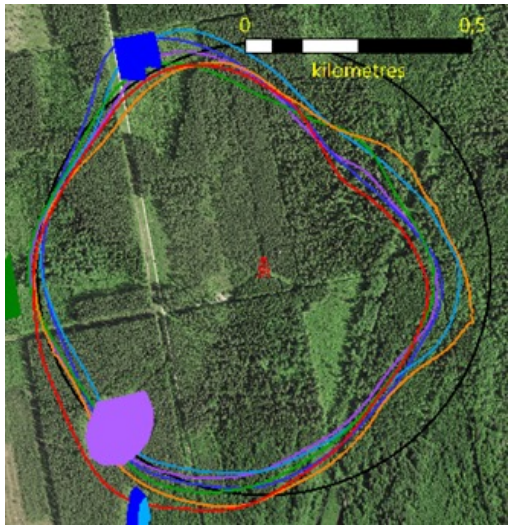

Figure 3. The contours of the FFP area for the years 2015–2020. It is visible that the change in the FFP area differs year to year and that these changes introduce also changes in the fraction of the land cover elements (e.g. clear-cut, road) or tree species. Coloured areas stand for clear-cuts. Blue, dark blue and purple colours show areas that were clear-cut in 2018, 2019 and 2020, respectively. The red sign in the middle indicates the location of the flux tower.

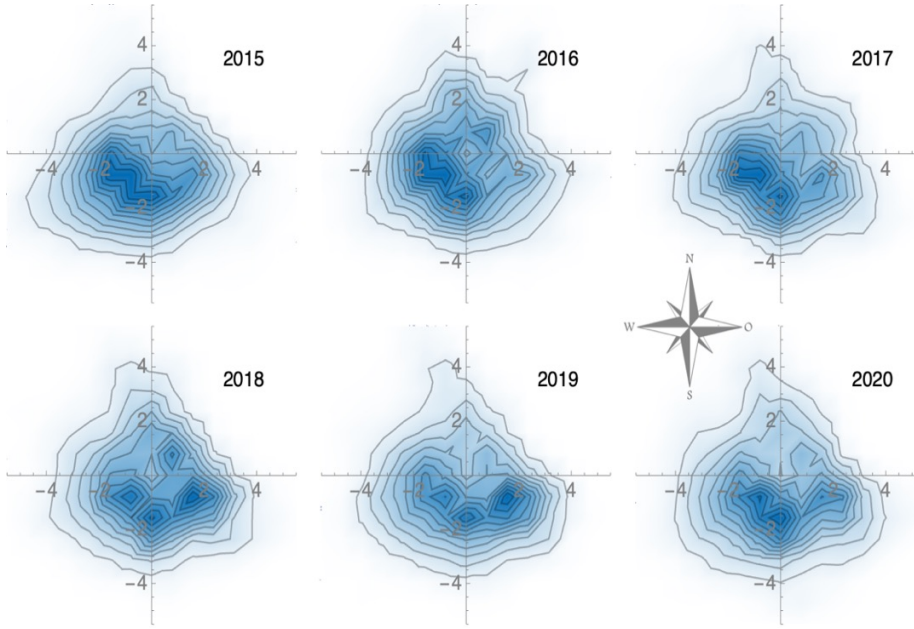

Figure 4. Heterogeneity in the annual wind direction and speed (m s^{-1}) measured at the SMEAR Estonia atmospheric tower at 30 m. The dominant wind directions ranged from the west to the south in 2015 to 2017 and in the more recent years from southwest to southeast. The darker colour on the figure denotes a higher density in wind direction and speed which means a higher contribution from those directions to the overall FFP.

by forests (Table 2). The main tree species growing in the area are the most widespread and economically most valuable species in Estonia: Scots pine (*Pinus sylvestris*) which cover 28.2 ha on average, silver and downy birch (*Betula spp.*) 6.8 ha on average, Norway spruce (*Picea abies*) 15.4 ha on average, common aspen (*Populus tremula*) 4.3 ha on average, grey (*Alnus incana* (L.) Moench) and black alder (*Alnus glutinosa* (L.) Gaertn.), 0.1 ha and 0.2 ha on average, respectively. Beside forest, there

are other land types in the FFP as well (Table 2), for example, power lines, buildings like the SMEAR main cottage and the shelter for power supply of the station, roads and ditches, and some clear areas and isles between the forest quarters. The main forest site types in the FFP are mineral dump, *Myrtillus, Uliginosum, Filipendula, Oxalis, Oxalis-Myrtillus, Oxycoccus* and drained swamp (Table 3).

Table 2. Land categories of the FFP area over the period of 2015–2020 at a height of 30 m.

Land type	Species	Area (ha)	Increment (m^3/ha/y)	Growing stock (m^3)	% of the FFP
Forest land	*Alnus incana*	0.1	0.5	7.6	0.2
Forest land	*Alnus glutinosa*	0.2	0.8	22.7	0.4
Forest land	*Populus tremula*	4.3	8.9	368.6	6.9
Forest land	*Betula* spp.	6.8	34.1	1179.5	11.1
Forest land	*Picea abies*	15.4	99.6	4234.5	25.0
Forest land	Pinus sylvestris	28.2	100.2	8448.0	45.8
Forest land	Unknown	2.8			
Isle in the forest	-	0.4			0.6
Buildings	-	0.0			0.0
Electric power lines	-	1.4			2.4
Roads	-	0.2			0.4
Ditches	-	0.6			1.0
Clear area	Clear-cut	1.0			1.6
Total	-	61.5			100.0
Total forest area	-	55.0			89.4

Table 3. Forest site types in the FFP measured at a height of 30 m.

Forest site type	2015	2016	2017	2018	2019	2020	Average area (ha)	% of FFP area	Average increment (m^3/ha/a)	% of FFP area	Average stock (m^3)	% of FFP area
Mineral dump	3.5	3.9	3.6	3.9	3.8	3.5	3.7	6.0				
Filipendula	8.4	8.6	9.1	8.8	9.0	8.8	8.8	14.3	35.9	14.7	1560.1	10.9
Oxalis	1.9	2.0	1.8	1.7	1.9	1.6	1.8	2.9	4.6	1.9	282.4	2.0
Oxalis-Myrtillus	1.5	3.2	2.6	2.8	1.9	2.1	2.3	3.8	16.0	6.5	660.0	4.6
Oxalis drained swamp	3.9	6.4	4.0	5.4	4.5	3.9	4.7	7.6	26.2	10.7	925.9	6.5
Myrtillus	22.8	22.9	22.0	22.3	22.8	21.2	22.3	36.3	99.8	40.9	6622.5	46.4
Uliginosum	14.2	13.1	11.7	12.7	12.4	12.2	12.7	20.7	45.9	18.8	2916.4	20.5
Oxycoccus	5.4	5.4	5.3	4.8	5.1	5.0	5.2	8.4	15.6	6.4	1293.5	9.1
Total	61.6	65.4	60.2	62.3	61.4	58.3	61.5	100.0	244.0	100.0	14260.9	100.0

Growing stocks and yearly increment were calculated for each year and are listed in Table 4. Depending on the year, the figures decreased or increased. The reasons for the decrease and increase might be different: 1) thinning and clear-cutting; 2) smaller/larger area of the FFP for a particular year. If the FFP is smaller, it means that the area where fluxes are detected from is closer to the flux tower. Therefore, the forest growing on the far edges of the FFP gets out of sight of the flux tower. Given there was no thinning/clear-cutting brought about the change in the growing stock perhaps due to shifting stands with different growing stock in or out of the FFP area. Thinning was done only in 2018 and 2019 when 273 m^3 and 501 m^3 were cut (Table 4), thus such small amounts had no significant impact on the shape of the FFP.

Table 4. Growing stock (m^3/ha) and increment (m^3/ha/y) changes during the six-year period.

Characteristic	Unit	Year					
		2015	2016	2017	2018	2019	2020
Area	ha	58.05	61.54	56.59	58.40	57.61	54.77
Stock in summer	m^3	13988	14732	14058	14558	14430	13799
Thinning & harvesting	m^3	0	0	0	273	501	
Increment	m^3	240	266	237	248	242	232
Stock in summer	m^3	14228	14998	14295	14533	14170	
Stock in summer	m^3/ha	240.98	239.39	248.40	249.29	250.45	251.91
Thinning	m^3/ha	0.00	0.00	0.00	4.68	8.70	
Increment	m^3/ha	4.13	4.32	4.18	4.24	4.19	4.24
Stock in next summer	m^3/ha	245.11	243.71	252.59	248.86	245.94	

The FFP description measured from a height of 70 m

The area of the FFP measured from a height of 70 m was significantly bigger (Figure 5) and covers the surrounding area of up to 4 km from the main tower. In 2015, the FFP covered 3,288 ha, in 2016 3,317.3 ha, in 2017 3,241.8 ha, in 2018 3,332.7 ha, in 2019 and 2020 the FFP covered areas of 3,323.8 ha and 3,272.3 ha, respectively. The average FFP area over the six-year period was 3,296 ha. The main shape of the FFP remained intact, although the FFP climatology were slightly different for each year as well as for the smaller 30 m FFP. The FFP area in 2016 was 0.9% bigger than in 2015, but in 2017 it was smaller by 2.3% than in 2016. In 2018, the area was again bigger than in 2017 by 2.8%, and the FFP area was again smaller in 2019 than in the previous year by 0.3%. In 2020, it was smaller by 1.6% than in 2019. On average, the difference over the years was only 1.6%. The main growing tree species in the FFP area are Scots pine (511.2 ha on average), silver and downy birch (1,007.9 ha on average), Norway spruce (450 ha on average), common aspen (242.7 ha on average), grey and black alder 37.4 ha and 464.5 ha on average, respectively. Bogs and fens cover 86 ha of the area and 40.7 ha of them are covered by Scots pine. Overall, 2,897.3 (87.9 %) ha of the FFP area is categorized as forest land, the remaining 398.7 ha are covered with different types of land (12.1 %) (Table 5). The main forest site types for this FFP are described in Table 6.

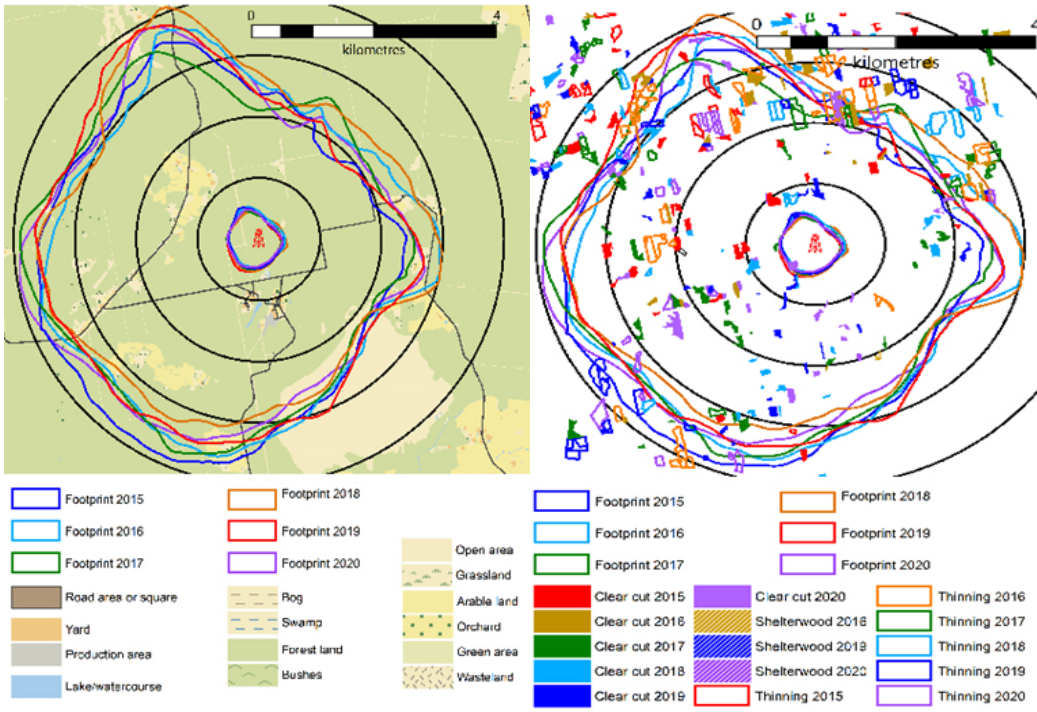

Figure 5. The contours of the FFP area in 2015–2020. It is visible that the change in the FFP area differs year to year and that these changes introduce also changes in the fraction of the land cover elements (e.g. clear-cut, road, forest area) or tree species. Different colours and filling patterns mark thinning and clear-cut areas in different years.

Table 5. Land categories of the FFP area over the period of 2015–2020 at a height of 70 m.

Land type	Species	Area (ha)	Increment (m^3/ha/y)	Growing stock (m^3)	% of FFP
Forest	*Alnus incana*	37.2	186.9	3251.9	1.1
Forest	*Alnus glutinosa*	464.5	1693.0	76381.2	14.1
Forest	*Populus tremula*	242.7	786.6	20652.5	7.4
Forest	*Betula* spp.	1007.9	3449.5	224027.0	30.6
Forest	*Picea abies*	450.0	2205.8	135347.7	13.7
Forest	*Pinus sylvestris*	470.5	1027.0	145716.4	14.3
Forest	Other species	0.1	0.1	58.0	0.0
Forest (bog)	*Pinus sylvestris*	40.7	52.5	1004.7	1.2
Forest	Clear-cut	183.6			5.6
Bog	Without forest	35.5			1.1
Fen	Without forest	9.8			0.3
Agricultural land	-	120.4			3.7
Clear area	-	83.8			2.5
Buildings	-	2.3			0.1

Land type	Species	Area (ha)	Increment (m^3/ha/y)	Growing stock (m^3)	% of FFP
Standing water	-	3.8			0.1
Isle in the forest	-	30.4			0.9
Roads	-	37.1			1.1
Watercourse	-	40.1			1.2
Yard	-	11.8			0.4
Other land	-	0.3			0.0
Power lines	-	23.5			0.7
Total forest land	-	2897.3			87.9
Total area	-	3296.0			100.0

Table 6. Forest site types in the FFP measured at a height of 70 m.

Forest site type	2015	2016	2017	2018	2019	2020	Average area (ha)	% of FFP	Average increment (m^3/ha/a)	% of FFP	Average stock (m^3)	% of FFP
Mineral dump	418.0	445.5	397.4	415.5	429.0	406.6	418.7	12.703				
Myrtillus	564.2	567.9	553.1	578.1	576.1	554.3	565.6	17.161	848.4	18.0	77460.9	25.4
Vaccinium	36.4	34.1	36.6	36.5	39.3	36.8	36.6	1.111	39.6	0.8	6332.8	2.1
Raised bog	42.9	45.7	36.2	25.3	52.6	18.0	36.8	1.116	19.5	0.4	414.8	0.1
Uliginosum	73.2	75.7	73.3	74.5	75.4	73.6	74.3	2.253	71.9	1.5	9110.2	3.0
Transitional bog	87.0	95.0	85.0	93.0	89.8	85.3	89.2	2.706	63.0	1.3	10211.7	3.3
Filipendula	1233.1	1254.7	1205.3	1296.9	1236.7	1231.0	1242.9	37.711	2024.0	42.9	122544.0	40.1
Oxalis	160.4	133.1	129.4	109.5	129.1	134.1	132.6	4.024	364.6	7.7	12762.4	4.2
Oxalis-Myrtillus	172.0	207.5	198.4	206.6	180.1	222.9	197.9	6.005	488.1	10.3	19911.9	6.5
Oxalis drained swamp	489.7	448.3	517.3	487.7	506.7	499.7	491.6	14.914	759.6	16.1	44217.1	14.5
Aegopodium	7.769	6.710	6.730	5.983	5.995	6.990	6.7	0.203	21.2	0.4	1866.7	0.6
Hepatica	2.982	2.982	2.982	2.982	2.982	2.982	3.0	0.090	21.2	0.4	414.6	0.1
Cladonia	0.280	0.000	0.222	0.000	0.000	0.000	0.1	0.003	0.1	0.0	21.9	0.0
Total							3296.0	100.0	4721.2	100.0	305268.8	100.0

Growing stocks were calculated for each year (Table 7), in some years the growing stock decreased or increased as compared to other years. The reasons behind these changes are similar to those given in the previous section.

Table 7. Growing stock (m^3/ha) and increment (m^3/ha/y) changes during the six-year period.

Characteristic	Unit	Year					
		2015	2016	2017	2018	2019	2020
Area	ha	2888.86	2891.82	2864.11	2938.29	2914.90	2886.02
Stock in summer	m^3	605713	603467	592571	618805	607847	610235
Thinning & harvesting	m^3	8481	10666	5577	9394	5943	
Increment	m^3	9187	9335	9134	9500	9551	9701
Stock in next summer	m^3	606418	602136	596127	618910	611455	
Stock in summer	m^3/ha	209.67	208.68	206.90	210.60	208.53	211.44
Thinning & harvesting	m^3/ha	2.94	3.69	1.95	3.20	2.04	
Increment	m^3/ha	3.18	3.23	3.19	3.23	3.28	3.36
Stock in next summer	m^3/ha	209.92	208.22	208.14	210.64	209.77	

At 70 m height, the dominant wind directions in 2015 to 2017 ranged from the southwest to south, like the 30 m anemometer measurements showed. In the more recent years, the general wind directions were also frequently from the south to southeast, but also northeast wind directions are prevalent at this height. The darker colour on the figure denotes a higher density in wind direction and speed and therefore a higher contribution from those directions to the overall FFP (Figure 6). Thus, wind speed and directions in those particular regions are more abundant which makes

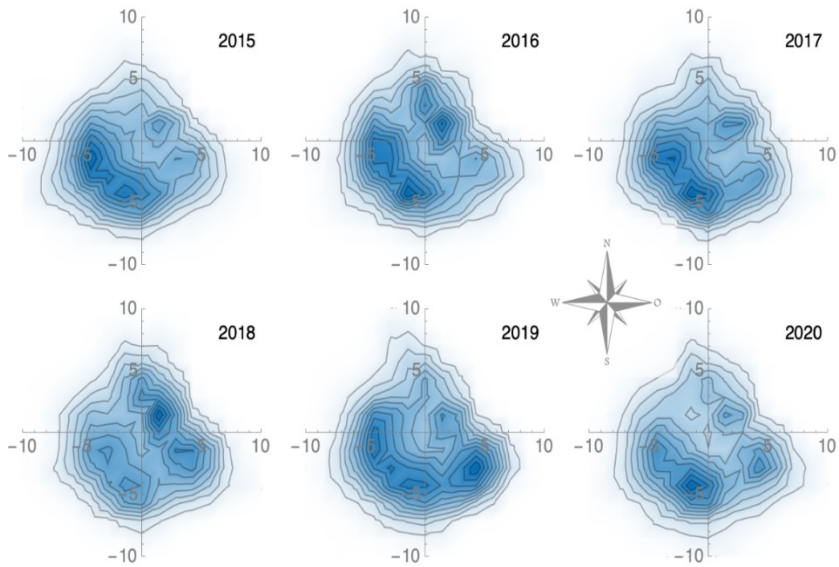

Figure 6. Heterogeneity in the annual wind direction and speed (m s^{-1}) measured at the SMEAR Estonia atmospheric tower at 70 m. The dominant wind directions ranged from the west to the south in 2015 to 2017 and in the more recent years from the southwest to the southeast. The darker colour on the figure denotes a higher density in wind direction and speed, which means a higher contribution from those directions to the overall FFP.

the input to calculate the overall FFP shape more robust.

Discussion

Average relative changes in the FFP area range about ~4.9% for the measurement height of 30 m and are smaller, 1.6%, for the measurement height of 70 m. This change is not controllable by human activity and follows the annual wind patterns. Changes that are affected by human activities, e.g. reduction in the growing stock after clear-cutting or thinning were also observed. The growing stock of the FFP area from 30 m height grew for 2.8% over the period reported. Since there were no construction activities next to the station, there were no land use changes regarding buildings, ditches, etc. and these structural elements of the FFP remained constant over the time observed.

For the FFP area at 70 m height, the value was 2.2% on average. Thinning took place every year and the impact of forest management activities might have had some effect on the shape of the FFP. We calculated the growing stock and increment for each year considering the thinning that was done and thus enabled a way to compare changes in the carbon stock of the FFP. Our comparisons reveal that in both FFPs the increment and growing stock have been constant over the 6 years.

The relative change over the years was smaller for the 70 m FFP compared to the 30 m FFP. Measurements from the higher point allow us therefore a more stable assessment in terms of the changes of forest management and other elements within the FFP. The shape of both FFPs is practically the same and shows some slight differences only. This indicates that the shape is driven by the larger scale wind regime and less by the local differences.

Relating the FFP areas and setting the 70 m FFP as 100%, the 30 m FFP covers only 3.4% of the whole area. Within the bigger area are therefore more land categories. For instance, bogs and swamps in the southeast part of the 70 m FFP contributed to it every year, but the size of that area was different. In that sense, the forested area in the 70 m FFP is more variable over the years as compared to the 30 m FFP. Another example are settlements and grassland that occurs in the eastern edge of the 70 m FFP, these elements are not apparent in the 30 m FFP. On the other hand, these changes at the border areas of the FFP have a very low effect given the FFP's transfer function's small weights for these areas. A benefit of the 70 m FFP is that we can study the impact of different land categories and forest management regimes on the carbon exchange. The smaller, 30 m FFP, has the disadvantage that the overall variation of the FFP area and changes like clear-cutting may lead to relatively large changes within the flux signature that may be captured in one year and left out in another year and by that complicating the proper assessment of the FFP area's carbon exchange over the years.

The application of wind data from the eddy covariance method described in this paper is an important and useful method for studying atmosphere-ecosystem relationships, fluxes of atmospheric gases and monitoring the LULUCF impacts on climate change mitigation strategies. It enables us to quantify changes in the FFP area that need consideration in assessing forest growth and linking it to climatic driven environmental changes. Utilising the SMEAR station's data is an important step towards understanding the FFP dynamic and to what extent environmental and human drivers affect changes in the forest ecosystem and how the ecosystem responds. Our work shows that the area of the FFP varies year by year due to wind speed and direction. Additionally, the anthropogenic impact of forest management on the land use elements in the FFP like cleared areas, changes in density by thinning, changes in height lead to an increased heterogeneity

in the FFP's three-dimensional structure. This heterogeneity modifies the FFP by impacting the turbulent flow field (Aubinet *et al.*, 2012). Such changes over time will impact the high-frequency losses that may be caused by the changing canopy surface roughness. Our findings confirmed that the overall change in the FFP area is relatively small and even if combined with the anthropogenic added up heterogeneity parameters like the standing stock or the yearly increment remained almost constant within the FFP area. This offers a possibility to study the effects of climate warming on the forest ecosystem carbon sink capacity while considering environmental and anthropogenic effects.

Conclusions

In this paper, we calculated the FFP measured at a height of 30 and 70 m in a hemiboreal mixed conifer and deciduous forest at the Järvselja Experimental Forestry Centre. The study provides a description of the dynamic changes within the FFP from 2015 to 2020. To assess the annual FFP climatology and the spatial extent of the FFP the EC method was used. Over the six-year period, the major shape of the FFP remained almost intact and all changes appeared mostly due to wind speed and direction. The wind direction was mainly from the south and southwest in 2015–2017 and from southeast in 2018–2020. Changes in the growing stock and increment were affected by forest management activities during the six-year period, however these changes were relatively small and constant over time.

Long-term measurements are crucial for understanding the relations between the forest ecosystem and the atmosphere. In this research paper we emphasize the importance of considering both natural and human factors when studying the dynamics of the FFP area, particularly in the context of climate change mitigation strategies. The use of advanced measurement methods and data from the SMEAR station is a valuable and useful tool for advancing our understanding of forest ecosystems and their response to changing environmental conditions and human activities.

Acknowledgements. The Estonian Research Council Grants PRG 1674, the Estonian Environmental Investment Centre (KIK) project number 18392 and the European Union's Horizon 2020 Research and Innovation programme (grant agreement no. 871115) ACTRIS IMP financed this study.

References

Amiro, B.D., Barr, A.G., Barr, J.G., Black, T.A., Bracho, R., Brown, M., Chen, J., Clark, K.L., Davis, K.J., Desai, A.R., Dore, S., Engel, V., Fuentes, J.D., Goldstein, A.H., Goulden, M.L., Kolb, T.E., Lavigne, M.B., Law, B.E., Margolis, H.A., Martin, T., McCaughey, J.H., Misson, L., Montes-Helu, M., Noormets, A., Randerson, J.T., Starr, G., Xiao, J. 2010. Ecosystem carbon dioxide fluxes after disturbance in forests of North America. – Journal of Geophysical Research: Biogeosciences, 115, G4. https://doi.org/10.1029/2010JG001390.

Aubinet, M., Vesala, T., Papale, D. 2012. Eddy Covariance. A Practical Guide to Measurement and Data Analysis. Dordrecht, Springer. 438 pp.

Baldocchi, D.D. 2003. Assessing the eddy covariance technique for evaluating carbon dioxide exchange rates of ecosystems: past, present and future. – Global Change Biology, 9(4), 479–492. https://doi.org/10.1046/j.1365-2486.2003.00629.x.

Baldocchi, D.D., Hincks, B.B., Meyers, T.P. 1988. Measuring biosphere-atmosphere exchanges of biologically related gases with micrometeorological methods. – Ecology, 69(5), 1331–1340. https://doi.org/10.2307/1941631.

Bourtsoukidis, E., Bonn, B., Noe, S.M. 2014. On-line field measurements of BVOC emissions from Norway spruce (*Picea abies*) at the hemiboreal SMEAR-Estonia site under autumn conditions. – Boreal Environmental Research, 19, 153–167.

Burba, G., Anderson, D., 2010. A Brief Practical Guide to Eddy Covariance Flux Measurements. Principles and Workflow Examples for Scientific and Industrial Applications. Lincoln, USA, LI-COR Biosciences. 213 pp.

Chu, H., Luo, X., Ouyang, Z., Chan, W.S., Dengel, S., Biraud, S.C., Torn, M.S., Metzger, S., Kumar, J., Arain, M.A., Arkebauer, T.J., Baldocchi, D., Bernacchi, C., Billesbach, D., Black, T.A., Blanken, P.D., Bohrer, G., Bracho, R., Brown, S., Brunsell, N.A., Chen, J., Chen, X., Clark, K., Desai, A.R., Duman, T., Durden, D., Fares, S., Forbrich, I., Gamon, J.A., Gough, C.M., Griffis, T., Helbig, M., Hollinger, D., Humphreys, E., Ikawa, H., Iwata, H., Ju, Y., Knowles, J.F., Knox, S.H., Kobayashi, H., Kolb, T., Law, B., Lee, X., Litvak, M., Liu, H., Munger, J.W., Noormets, A., Novick, K., Oberbauer, S.F., Oechel, W., Oikawa, P., Papuga, S.A., Pendall, E., Prajapati, P., Prueger, J., Quinton, W.L., Richardson, A.D., Russell, E.S., Scott, R.L., Starr, G., Staebler, R., Stoy, P.C., Stuart-Haëntjens, E., Sonnentag, O., Sullivan, R.C., Suyker, A., Ueyama, M., Vargas, R., Wood, J.D., Zona, D. 2021. Representativeness of Eddy-Covariance flux footprints for areas surrounding AmeriFlux sites. – Agricultural and Forest Meteorology, 301–302, 108350.

Ezhova, E., Ylivinkka, I., Kuusk, J., Komsaare, K., Vana, M., Krasnova, A., Noe, S., Arshinov, M., Belan, B., Park, S.-B., Lavrič, J.V., Heimann, M., Petäjä, T., Vesala, T., Mammarella, I., Kolari, P., Bäck, J., Rannik, Ü., Kerminen, V.-M., Kulmala, M. 2018. Direct effect of aerosols on solar radiation and gross primary production in boreal and hemiboreal forests. – Atmospheric Chemistry and Physics, 18(24), 17863–17881. https://doi.org/10.5194/acp-18-17863-2018.

Finnigan, J.J. 2004. A re-evaluation of long-term flux measurement techniques part II: coordinate systems. – Boundary-Layer Meteorology, 113, 1–41.

Forest Inventory Act. 2009. Metsa korraldamise juhend. – RT I, 22.02.2017, 10. [WWW document]. – URL https://www.riigiteataja.ee/akt/13124148?leiaKehtiv. [Accessed 12 December 2023]. (In Estonian).

Hari, P., Kulmala, L. 2008. Boreal Forest and Climate Change. Dordrecht, Springer. 582 pp.

Hari, P., Andreae, M.O., Kabat, P., Kulmala, M. 2009. A comprehensive network of measuring stations to monitor climate change. – Boreal Environment Research, 14, 442–446.

Keenan, T.F., Prentice, I.C., Canadell, J.G., Williams, C.A., Wang, H., Raupach, M., Collatz, G.J. 2016. Recent pause in the growth rate of atmospheric CO_2 due to enhanced terrestrial carbon uptake. – Nature Communications, 7, 13428. https://doi.org/10.1038/ncomms13428.

Kiviste, K., Kiviste, A. 2009. Algebraic difference equations for stand height, diameter, and volume depending on stand age and site factors for Estonian state forests. – Mathematical and Computational Forestry & Natural-Resource Science, 1(2), 67–77.

Kljun, N., Calanca, P., Rotach, M.W., Schmid, H.P. 2004. A simple parameterisation for flux footprint predictions. – Boundary-Layer Meteorology, 112, 503–523. https://doi.org/10.1023/B:BOUN.0000030653.71031.96.

Kljun, N., Calanca, P., Rotach, M.W., Schmid, H.P. 2015. A simple two-dimensional parameterisation for Flux Footprint Prediction (FFP). – Geoscientific Model Development, 8(11), 3695–3713. https://doi.org/10.5194/gmd-8-3695-2015.

Kollo, J., Metslaid, S., Padari, A., Hordo, M., Kangur, A., Noe, S.M. 2023. Trends in thermal growing season length from years 1955–2020 – A case study in hemiboreal forest in Estonia. – Boreal Environment Research, 28, 169–180.

Kulmala, M. 2016. On COBACC (COntinental Biosphere-Aerosol-Cloud-Climate) feedback. – Geophysical Research Abstracts, Volume 18. Vienna, EGU General Assembly. EGU2016-16372.

Kulmala, M., Nieminen, T., Nikandrova, A., Lehtipalo, K., Manninen, H.E., Kajos, M.K., Kolari, P., Lauri, A., Petäjä, T., Krejci, R., Hansson, H.-C., Swietlicki, E., Lindroth, A., Christensen, T.R., Arneth, A., Hari, P., Bäck, J., Vesala, T., Kerminen, V.-M. 2014. CO_2-induced terrestrial climate feedback mechanism: From carbon sink to aerosol source and back. – Boreal Environment Research, 19, 122–131.

Lang, M., Kaha, M., Laarmann, D., Sims, A. 2018. Construction of tree species composition map of Estonia using multispectral satellite images, soil map and a random forest algorithm. – Forestry Studies / Metsanduslikud Uurimused 68, 5–24.

Maa-amet. 2017. Estonian Topographic Data Collection. (Eesti topograafia andmekogu). [WWW document]. – URL https://geoportaal.maaamet.ee/est/ruumiandmed/eesti-topograafia-andmekogu-p79.html. [Accessed 12 December 2023]. (In Estonian).

Mäki, M., Krasnov, D., Hellén, H., Noe, S.M., Bäck, J. 2019. Stand type affects fluxes of volatile organic compounds from the forest floor in hemiboreal and boreal climates. – Plant and Soil, 441, 363–381. https://doi.org/10.1007/s11104-019-04129-3.

Noe, S.M., Kimmel, V., Hüve, K., Copolovici, L., Portillo-Estrada, M., Püttsepp, Ü., Jõgiste, K., Niinemets, Ü., Hörtnagl, L., Wohlfahrt, G. 2011. Ecosystem-scale biosphere-atmosphere interactions of a hemiboreal mixed forest stand at Järvselja, Estonia. – Forest Ecology Management, 262(2), 71–81. https://doi.org/10.1016/j.foreco.2010.09.013.

Noe, S.M., Krasnov, D., Krasnova, A., Cordey, H.P.E., Niinemets, Ü. 2016. Seasonal variation and characterisation of reactive trace gas mixing ratios over a hemi-boreal mixed forest site in Estonia. – Boreal Environment Research, 21, 332–344.

Noe, S.M., Krasnova, A., Krasnov, D., Cordey, H.P.E., Kangur, A. 2021. Facilitating long-term 3D sonic anemometer measurements in hemiboreal forest ecosystems. – Forestry Studies / Metsanduslikud Uurimused, 75, 140–149. https://doi.org/10.2478/fsmu-2021-0016.

Noe, S.M., Niinemets, Ü., Krasnova, A., Krasnov, D., Motallebi, A., Kängsepp, V., Jõgiste, K., Hõrrak, U., Komsaare, K., Mirme, S., Vana, M., Tammet, H., Bäck, J., Vesala, T., Kulmala, M., Petäjä, T., Kangur, A. 2015. SMEAR Estonia: Perspectives of a large-scale forest ecosystem – atmosphere research infrastructure. – Forestry Studies / Metsanduslikud Uurimused, 63, 56–84.

Rebane, S., Jõgiste, K., Kiviste, A., Stanturf, J.A., Metslaid, M. 2020. Patterns of carbon sequestration in a young forest ecosystem after clear-cutting. – Forests, 11(2), 126. https://doi.org/10.3390/f11020126.

Schmid, H.P. 2002. Footprint modeling for vegetation atmosphere exchange studies: a review and perspective. – Agricultural and Forest Meteorology, 113(1–4), 159–183. https://doi.org/10.1016/S0168-1923(02)00107-7.

Spracklen, D.V., Jimenez, J.L., Carslaw, K.S., Worsnop, D.R., Evans, M.J., Mann, G.W., Zhang, Q., Canagaratna, M.R., Allan, J., Coe, H., McFiggans, G., Rap, A., Forster, P. 2011. Aerosol mass spectrometer constraint on the global secondary organic aerosol budget. – Atmospheric Chemistry and Physics, 11(23), 12109–12136. https://doi.org/10.5194/acp-11-12109-2011.

Teets, A., Fraver, S., Hollinger, D.Y., Weiskittel, A.R., Seymour, R.S., Richardson, A.D. 2018. Linking annual tree growth with eddy-flux measures of net ecosystem productivity across twenty years of observation in a mixed conifer forest. – Agricultural and Forest Meteorology, 249, 479–487. https://doi.org/10.1016/j.agrformet.2017.08.007.

Vesala, T., Kljun, N., Rannik, Ü., Rinne, J., Sogachev, A., Markkanen, T., Sabelfeld, K., Foken, T., Leclerc, M.Y. 2008. Flux and concentration footprint modelling: State of the art. – Environmental Pollution, 152(3), 653–666. https://doi.org/10.1016/j.envpol.2007.06.070.

Zhong, W., Haigh, J.D. 2013. The greenhouse effect and carbon dioxide. – Weather, 68(4), 100–105. https://doi.org/10.1002/wea.2072.